Supplementary Information for:
Oxygen Solubility and Transport in Li-Air Battery Electrolytes: Establishing Criteria and Strategies for Electrolyte Design

Forrest S. Gittleson*, Reese E. Jones, Donald K. Ward, Michael E. Foster
Sandia National Laboratories, Livermore, CA 94550, USA

Electrochemically Active Surface Area (ECSA) Calculation

The ECSA of Sigracet 25BC carbon electrodes was measured capacitatively using a symmetric cell with two 15 mm diameter electrodes sandwiching a separator impregnated with 60 µL 1M LiTFSI/Pyr$_{14}$TFSI (1-butyl-1-methylpyrrolidinium bis(trifluoromethanesulfonyl)imide). After 800 cycles in the range 0-0.8 V at a rate of 15.7 µA, a capacitance of ~5900 µF was obtained.

As shown by Zhang et al.,[1] the specific capacitance of sp^2 carbon materials can be related to the effective specific surface area (a.k.a. electrochemically active surface area) with the equation:

$$C = \varepsilon \varepsilon_0 A / d$$

Where ε is the relative dielectric constant of the electrolyte, ε_0 is the vacuum permittivity (8.85 x 10^{-12} F/m), A is the surface area and d is the thickness of the electric double layer (the distance between the center of the interacting species and pore wall). While Zhang et al. prove the correlation using imidazolium-based ionic liquids, we employ Pyr$_{14}$TFSI which has a permittivity (ε) of 11.7.[2] If we assume O$_2$ molecules (~1.5 Å radius) interact at the electrode surface rather than Pyr$_{14}^+$ (~3.4 Å radius) or Li$^+$ (~0.9 Å radius) ions, then we can use d = 1.5 Å. This assumption is reasonable given the one electron limiting reaction during discharge in our Li-air cell (O$_2$ + e$^-$ ↔ O$_2^-$). With the experimentally determined capacitance and equation above, we calculate A = 83 cm^2 per 15 mm diameter Sigracet 25BC electrode.

Electrochemical Methods for Determining D(O$_2$) and C(O$_2$)

Several electrochemical methods exist to determine the diffusion coefficient and concentration of a redox active solute in solution. Li-O$_2$ chemistry, however, has unique challenges that limit the accuracy of some methods. In particular, the tendency of insulating reduction products to precipitate and passivate an electrode makes certain stagnant electrolyte techniques difficult to implement with confidence. Both the Cottrell method using chronoamperometry and the Randles-Sevcik/Nicholson-Shain method using cyclic voltammetry in stagnant electrolytes[3] are prone to error from rapidly accumulating solid products. Furthermore, these techniques are likely to induce convection in the electrolyte at longer time scales, which will negatively influence the analysis.[4] The use of a microelectrode is able to limit some of these undesired affects, but electrode passivation is still a concern.[5]

Both the Levich technique and hydrodynamic chronocoulometry[6,7] using rotating disc or rotating ring disc electrodes make use of controlled electrolyte convection. By rapidly sweeping the semi-soluble Li-O$_2$ reduction intermediates from a flat disc electrode, passivation can be reduced vs. stagnant electrolyte experiments. Since the Levich equation includes terms for both concentration and diffusion coefficient, it is unreliable to determine both parameters from the same set of data.

Hydrodynamic chronocoulometry attempts to solve this by determining the diffusion coefficient and concentration from different aspects of the same data set. The tactic we employ in this work is to independently determine $D(O_2)$ from the transit time method using a rotating ring disc electrode[8] and $C(O_2)$ using the Levich method (examples in Fig. S8b,d,f,g). We believe this methodology provides additional confidence in $D(O_2)$ and $C(O_2)$ measurements for Li^+ electrolytes compared to previous reports. Reported literature values for $D(O_2)$ in lithium and tetraalkylammonium electrodes using some of these methods are found in Table S5 and compare favorably to the values derived in this work.

A final note considers the use of commercial dissolved oxygen meters which employ galvanic techniques.[9–11] Since these tools are typically calibrated for use in aqueous solutions, the quality of $C(O_2)$ data for non-aqueous solutions should be viewed as highly suspect, particularly with lithium chemistries.

Supplemental Figures
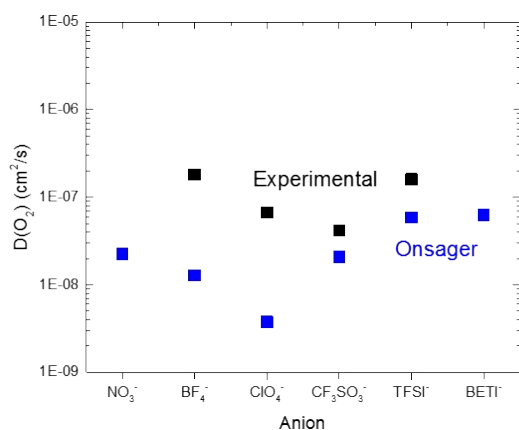
Figure S1. Calculated Onsager diffusion coefficients for oxygen in 1M LiX/TEGDME electrolytes from molecular dynamics simulation with comparison to experimental values.
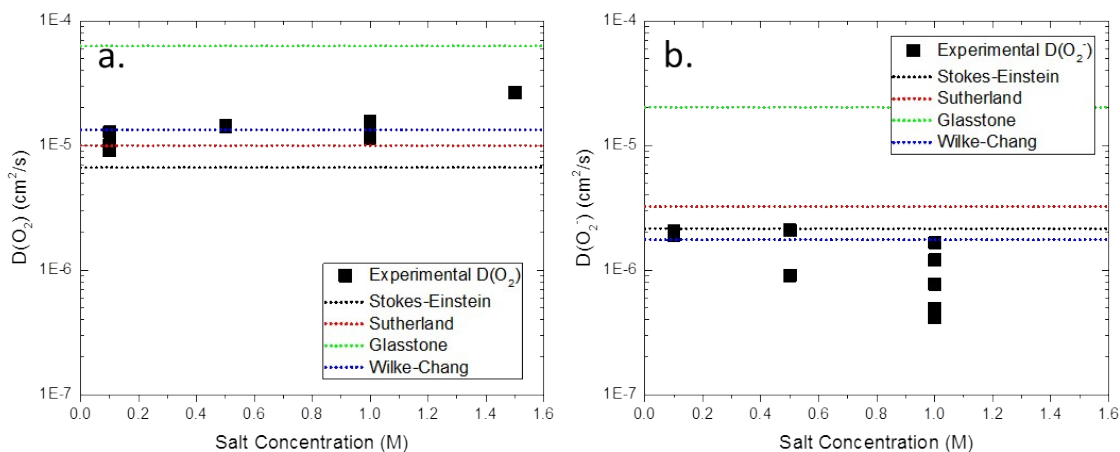
Figure S2. Comparison of experimentally derived diffusion coefficients (a) $D(O_2)$ and (b) $D(O_2^-)$ and viscosity-diffusion models for dilute DMSO electrolyte solutions.

Several diffusion models have been used to predict the diffusion coefficient of solutes in dilute solutions.[12] These equations and the parameters we used to calculate $D(O_2)$ and $D(O_2^-)$ as a function of viscosity, η, for dilute solutions of DMSO are shown below.

Models	*Basic equation*	
Stokes-Einstein	$D = \dfrac{k_B T}{6\pi\eta R_0}$	
Sutherland	$D = \dfrac{k_B T}{4\pi\eta R_0}$	(Non-stick solute surface)
Glassstone	$D = \dfrac{k_B T}{2\eta R_0}$	(Diffusion as a rate process)
Wilke-Chang	$D = \dfrac{7.4 \times 10^{-8}(\varphi M_2)^{1/2}T}{\eta V_1^{0.6}}$	(Empirical)

Parameters
$k_B = 1.38 \times 10^{-23}$ m^2 kg/s^2 K (Boltzmann constant)
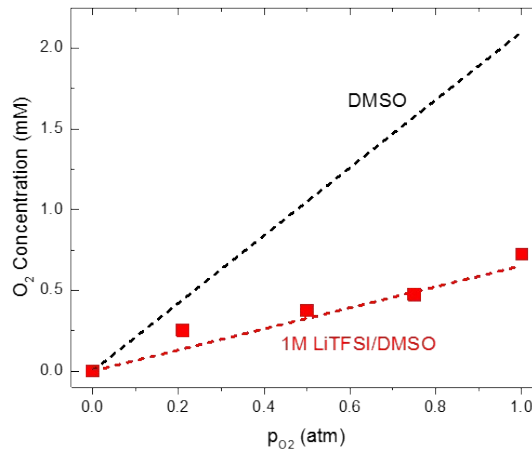$T = 295$ K
$R_0 = 1.5 \times 10^{-10}$ m (radius of O_2)
$R_0 = 4.9 \times 10^{-10}$ m (radius of $O_2^-[DMSO]_6$)
$\varphi = 1.0$ (factor for non-hydrogen bonded solvents, i.e. DMSO)
$M_2 = 78.13$ g/mol (molecular weight of DMSO)
$V_1 = 25.6$ cm^3/g mol (molal volume of O_2 at boiling point)
$V_1 = 751.3$ cm^3/g mol (estimated molal volume of O_2^- at boiling point, corrected for solvated volume of $O_2^-[DMSO]_6$)

Figure S3. Oxygen concentration vs. partial pressure in 1M LiTFSI/DMSO. Experimental values were derived from Levich analyses. Dotted lines represent Henry's law correlation between partial pressure and concentration for pure DMSO (black) and a linear fit from experiment for 1M LiTFSI/DMSO (red).
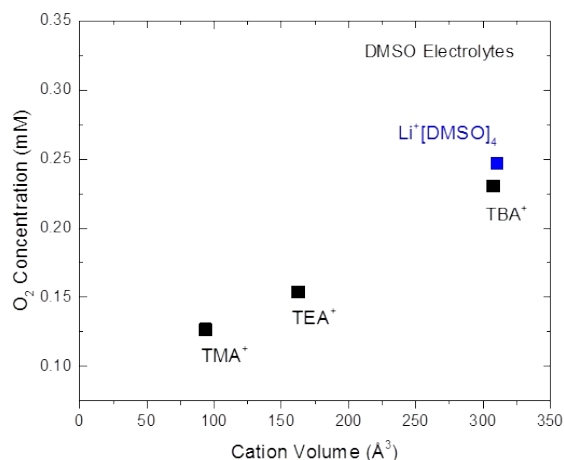
Figure S4. Oxygen concentration as a function of cation volume in 0.1M X-BF$_4$/DMSO electrolytes. Tetramethylammonium (TMA$^+$), tetraethylammonium (TEA$^+$) and tetrabutylammonium (TBA$^+$) are used as cations. Note that fully solvated Li$^+$[DMSO]$_4$ fits with the trend of tetraalkylammonium cations.
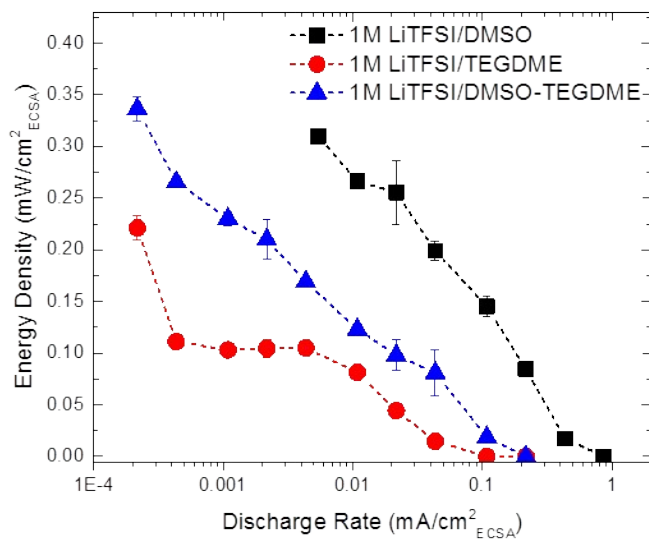
Figure S5. Energy density as a function of discharge rate to accompany Figure 6.
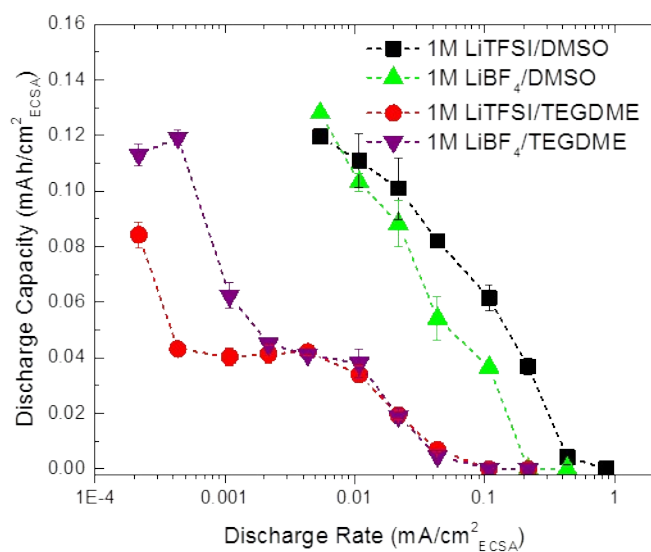
Figure S6. Discharge capacity for various electrolyte compositions as a function of discharge rate.

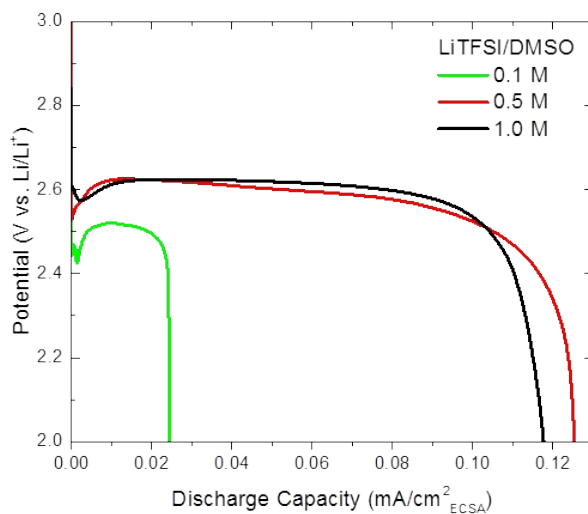**Figure S7.** Discharge profiles for LiTFSI/DMSO electrolytes showing the impact of the Li^+ diffusion limit at low Li^+ concentration. All cells are discharged at 108 $\mu A/cm^2_{ECSA}$, which is lower than calculated $i_{lim}(O_2)$ values and $i_{lim}(Li^+)$ values for 0.5M and 1M but higher than the calculated $i_{lim}(Li^+)$ value for 0.1M. This implies that at this current rate, a cell with a 0.1M LiTFSI/DMSO electrolyte is Li^+ transport limited.

5
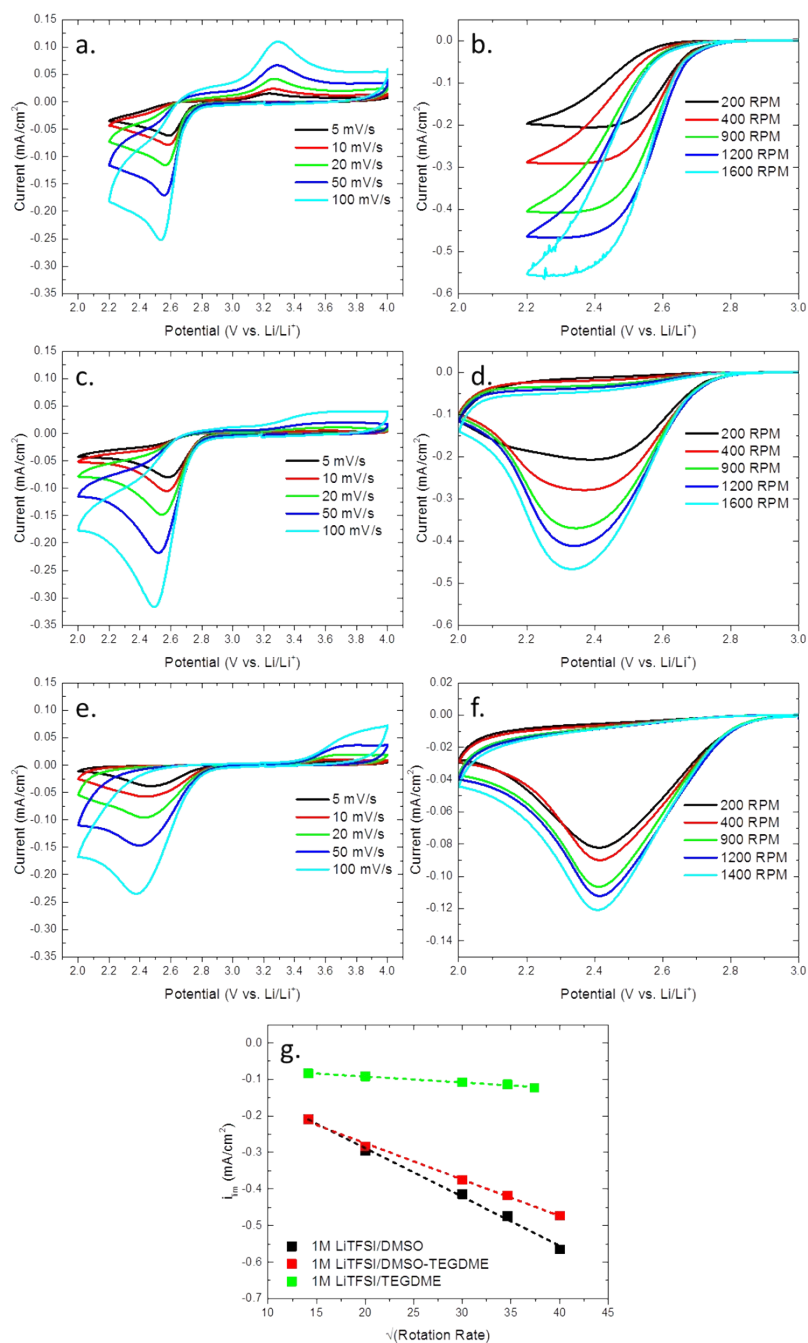
Figure S8. Cyclic voltammograms of a glassy carbon electrode in a stagnant electrolyte purged with dry air at various scan rates for (a) 1M LiTFSI/DMSO, (c) 1M LiTFSI/DMSO-TEGDME and (e) 1M LiTFSI/TEGDME. Cyclic voltammograms of the oxygen reduction region with a glassy carbon electrode at various rotation rates and 10 mV/s scan rate for (b) 1M LiTFSI/DMSO, (d) 1M LiTFSI/DMSO-TEGDME and (f) 1M LiTFSI/TEGDME. (g) Levich plot for data in (b, d, f) taken at the mass transport-limited plateau or peak (i_{lim}). Note that even in electrolytes which demonstrate a reduction "peak" rather than a mass transport-limited "plateau," the Levich correlation between i_{lim} and $\omega^{1/2}$ holds.

6

M	Electrolyte	ρ_{exp} (g/cm^3)	ρ_{calc} (g/cm^3)	D(O$_2$) Onsager cm^2/s	Fick cm^2/s	Experimental cm^2/s
1	LiNO$_3$/DMSO	1.151	1.156	1.10E-07	6.49E-05	1.44E-05
1	LiBF$_4$/DMSO	1.173	1.154	1.39E-07	2.29E-04	1.55E-05
1	LiClO$_4$/DMSO	1.171	1.184	1.25E-07	6.46E-05	1.24E-05
1	LiCF$_3$SO$_3$/DMSO	1.179	1.184	8.38E-08	4.15E-05	1.14E-05
1	LiTFSI/DMSO	1.217	1.256	7.99E-08	1.70E-04	1.09E-05
1	LiBETI/DMSO	1.246	1.277	5.31E-08	1.98E-05	1.18E-05
1	LiNO$_3$/TEGDME			2.24E-08		
1	LiBF$_4$/TEGDME	1.085	1.12	1.29E-08		1.81E-07
1	LiClO$_4$/TEGDME	1.084	1.14	3.78E-09		6.72E-08
1	LiCF$_3$SO$_3$/TEGDME	1.103	1.104	2.07E-08		4.17E-08
1	LiTFSI/TEGDME	1.168	1.13	5.88E-08		1.60E-07
1	LiBETI/TEGDME			6.27E-08		

Table S1. Calculated diffusion coefficients from molecular dynamics simulation. Calculated densities are within 4 % of experimental values.

p$_{O2}$ atm	D(O$_2$) cm^2/s	D(O$_2^-$) cm^2/s	C(O$_2$) mM
0			0
0.21	1.09E-05	4.94E-07	0.252
0.50	1.45E-05	9.70E-07	0.376
0.75	1.09E-05	1.25E-06	0.474
1.00	1.00E-05	1.24E-06	0.723

Table S2. O$_2$ diffusion coefficient and concentration as a function of O$_2$ partial pressures (from O$_2$/N$_2$ mixtures) in 1M LiTFSI/DMSO.

M	Electrolyte	ΔG_{solv} kcal/mol K	k_H atm	C(O$_2$)$_{calc}$ mM	C(O$_2$)$_{exp}$ mM
1	LiNO$_3$/DMSO	1.460441	4344.704	0.717201	0.119
1	LiBF$_4$/DMSO	0.95073	1816.494	1.711998	0.123
1	LiClO$_4$/DMSO	1.298261	3247.475	0.945952	0.135
1	LiCF$_3$SO$_3$/DMSO	1.204163	2673.998	1.110776	0.178
1	LiTFSI/DMSO	0.912429	1519.275	1.827666	0.252
1	LiBETI/DMSO	0.936561	1511.823	1.753909	0.258

Table S3. Free energies of solvation, Henry's law constants and oxygen concentrations from 1 atm air calculated from molecular dynamics simulation.

M	Electrolyte	σ	t_{Li}	$D(Li^+)^*$	$D(O_2)$	$i_{lim}(Li^+)^*$	$i_{lim}(O_2)^{**}$
		mS/cm		cm²/s	cm²/s	mA/cm²	mA/cm²
1.0	LiNO$_3$/DMSO	6.06	0.82	1.40E-07	1.44E-05	3.32E-02	1.41E-02
0.1	LiBF$_4$/DMSO	1.56	0.85	3.70E-07	1.01E-05	8.79E-03	2.06E-02
0.5	LiBF$_4$/DMSO	4.32	0.88	2.12E-07	1.46E-05	2.52E-02	1.77E-02
1.0	LiBF$_4$/DMSO	6.54	0.85	1.56E-07	1.55E-05	3.70E-02	1.57E-02
1.0	LiClO$_4$/DMSO	7.45	0.89	1.85E-07	1.24E-05	4.39E-02	1.37E-02
1.0	LiCF$_3$SO$_3$/DMSO	9.22	0.95	2.46E-07	1.14E-05	5.83E-02	1.66E-02
0.1	LiTFSI/DMSO	1.56	0.85	3.70E-07	1.28E-05	8.79E-03	2.46E-02
0.5	LiTFSI/DMSO	4.32	0.88	2.12E-07	1.40E-05	2.52E-02	2.40E-02
1.0	LiTFSI/DMSO	7.40	0.88	1.82E-07	1.09E-05	4.33E-02	2.26E-02
0.1	LiBETI/DMSO	0.97	0.84	2.29E-07	9.10E-06	5.44E-03	2.13E-02
0.5	LiBETI/DMSO	1.69	0.81	7.64E-08	1.44E-05	9.06E-03	2.65E-02
1.0	LiBETI/DMSO	5.33	0.74	1.11E-07	1.18E-05	2.63E-02	2.50E-02
1.0	LiBF$_4$/TEGDME	0.60	0.89	1.50E-08	1.81E-07	3.55E-03	-
1.0	LiClO$_4$/TEGDME	0.63	0.88	1.57E-08	6.72E-08	3.72E-03	-
1.0	LiCF$_3$SO$_3$/TEGDME	0.58	0.92	1.49E-08	4.17E-08	3.55E-03	-
0.1	LiTFSI/TEGDME	0.21	0.70	4.08E-08	1.13E-07	9.69E-04	6.72E-04
0.5	LiTFSI/TEGDME	1.37	0.69	5.28E-08	3.97E-07	6.26E-03	1.46E-03
1.0	LiTFSI/TEGDME	1.61	0.76	3.44E-08	1.60E-07	8.15E-03	7.87E-04
1.0	LiTFSI/DMSO-TEGDME	1.89	0.88	4.63E-08	8.07E-06	1.10E-02	1.69E-02

* Assumes diffusion with 2.7 V driving force and δ_O, the thickness of the separator plus half of the porous electrode (337.5 μm), ** Assumes 1 atm air at 295 K with $C(O_2)$ from Table 1 and δ_O, the thickness of half the porous electrode (117.5 μm)

Table S4. Comparison of ionic conductivity σ, transference number t_{Li}, and calculated i_{lim} values for Li$^+$-limited and O$_2$-limited cases. Calculated i_{lim} values (for Li$^+$ or O$_2$) that dictate cell dynamics are highlighted in red.

	Electrolyte	$D(O_2)$	$D(O_2^-)$	Refs
M		cm^2/s	cm^2/s	
Lithium Electrolytes				
0.1	LiPF$_6$/DMSO	1.67E-05		3
0.1	LiPF$_6$/CH$_3$CN	4.64E-06		3
0.1	LiPF$_6$/CH$_3$CN	3.77E-07		13
0.1	LiPF$_6$/DME	1.22E-05		3
0.1	LiPF$_6$/TEGDME	2.17E-06		3
Alkylammonium Electrolytes				
0.1	TBA-PF$_6$/DMSO	9.75E-06		3
0.1	TBA-PF$_6$/DMSO	2.20E-05	3.60E-07	5
0.1	TBA-ClO$_4$/DMSO	3.05E-05		14
0.1	TBA-ClO$_4$/DMSO	2.30E-05	4.68E-06	5
0.1	TBA-CF$_3$SO$_3$/DMSO	1.80E-05	1.65E-06	5
0.1	TBA-TFSI/DMSO	4.70E-05	4.21E-06	5
0.1	TEA-ClO$_4$/DMSO	2.08E-05		7
0.1	TEA-ClO$_4$/DMSO	3.23E-05		15
0.1	TMA-BF$_4$/DMSO	2.72E-05	2.55E-06	This work*
0.1	TEA-BF$_4$/DMSO	1.89E-05	5.18E-06	This work*
0.1	TBA-BF$_4$/DMSO	1.14E-05	3.25E-06	This work*
0.1	TBA-PF$_6$/CH$_3$CN	2.10E-05	9.00E-06	3,13
0.1	TBA-ClO$_4$/CH$_3$CN	2.30E-05	8.40E-06	13
0.1	TEA-ClO$_4$/CH$_3$CN	7.21E-05		7
0.1	TBA-PF$_6$/DME	3.88E-06		3
0.1	TBA-PF$_6$/DME	1.79E-04		16
0.1	TBA-ClO$_4$/DME	1.82E-04		16
0.1	TBA-CF$_3$SO$_3$/DME	1.58E-04		16
0.1	TBA-TFSI/DME	1.75E-04		16
0.1	TBA-CF$_3$SO$_3$/TEGDME	3.50E-05		16

*These values derived using 1 atm dry air.

Table S5. Diffusion coefficients of O_2 with lithium and alkylammonium electrolytes from literature.

References

1   L. Zhang, X. Yang, F. Zhang, G. Long, T. Zhang, K. Leng, Y. Zhang, Y. Huang, Y. Ma, M. Zhang and Y. Chen, *J. Am. Chem. Soc.*, 2013, **135**, 5921−5929.

2   H. Weingärtner, P. Sasisanker, C. Daguenet, P. J. Dyson, I. Krossing, J. M. Slattery and T. Schubert, *J. Phys. Chem. B*, 2007, **111**, 4775–4780.

3   C. O. Laoire, S. Mukerjee, K. M. Abraham, E. J. Plichta and M. A. Hendrickson, *J. Phys. Chem. C*, 2010, **114**, 9178–9186.

4   M. Chatenet, M. B. Molina-Concha, N. El-Kissi, G. Parrour and J. P. Diard, *Electrochim. Acta*, 2009, **54**, 4426–4435.

5   I. Gunasekara, S. Mukerjee, E. J. Plichta, M. A. Hendrickson and K. M. Abraham, *J. Electrochem. Soc.*, 2014, **161**, A381−A392.

6   S. E. Morris, *Trends Anal. Chem.*, 1988, **7**, 227–232.

7   M. Tsushima, K. Tokuda and T. Ohsaka, *Anal. Chem.*, 1994, **66**, 4551–4556.

8   F. Gan and D.-T. Chin, *J. Appl. Electrochem*, 1993, **23**, 452–455.

9   W. Xu, J. Xiao, J. Zhang, D. Wang and J.-G. Zhang, *J. Electrochem. Soc.*, 2009, **156**, A773–A779.

10   W. Xu, J. Xiao, D. Wang, J. Zhang and J.-G. Zhang, *J. Electrochem. Soc.*, 2010, **157**, A219–A224.

11   W. Xu, J. Hu, M. H. Engelhard, S. A. Towne, J. S. Hardy, J. Xiao, J. Feng, M. Y. Hu, J. Zhang, F. Ding, M. E. Gross and J.-G. Zhang, *J. Power Sources*, 2012, **215**, 240–247.

12   E. L. Cussler, *Diffusion: Mass Transfer in Fluid Systems*, Cambridge University Press, Cambridge, UK, 1997.

13   C. O. Laoire, S. Mukerjee, K. M. Abraham, E. J. Plichta and M. A. Hendrickson, *J. Phys. Chem. C*, 2009, **113**, 20127–20134.

14   D. Vasudevan and H. Wendt, *J. Electroanal. Chem.*, 1995, **192**, 69–74.

15   D. T. Sawyer and J. L. Roberts, *J. Electroanal. Chem.*, 1966, **12**, 90–101.

16   I. Gunasekara, S. Mukerjee, E. J. Plichta, M. A. Hendrickson and K. M. Abraham, *J. Electrochem. Soc.*, 2015, **162**, A1055−A1066.